Carbon Letters (2021) 31:941–956
https://doi.org/10.1007/s42823-020-00205-2

Online ISSN 2233-4998
Print ISSN 1976-4251

ORIGINAL ARTICLE

Preparation and characterization of chars and activated carbons from wood wastes

Qiangu Yan[1] · Jinghao Li[2] · Zhiyong Cai[2]

Received: 22 August 2020 / Revised: 15 October 2020 / Accepted: 5 November 2020 / Published online: 22 November 2020

Abstract

Preparation of activated carbons from wood waste including northern hardwood pins-fines and wood dust was conducted and then compared through the following methods: physical pyrolysis and CO_2 activation, vacuum pyrolysis and CO_2 activation, CO_2 gasification, and vacuum CO_2 gasification processes. Experimental results show that chars and activated carbons with high surface area and pore volume are produced from wood waste through a vacuum CO_2 pyrolysis/gasification process. The effects of operation variables of vacuum pyrolysis/gasification on the properties of chars and activated carbons were investigated to identify and optimize the temperature, heating time, and heating rate. The optimized vacuum CO_2 gasification conditions were found to be a temperature of 800 °C, a heating rate of 20 °C/min, and a holding time of 2 h respectively. The prepared wood-chars and activated carbons were characterized by nitrogen physisorption, scanning electron microscopy (SEM). Fourier transform infrared (FTIR) spectra determined any changes in the surface functional groups produced during different preparation stages.

Graphic abstract

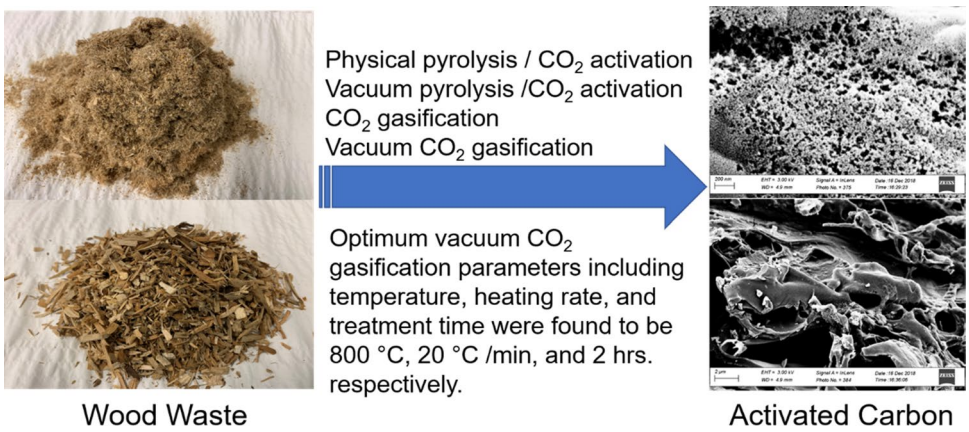

Keywords Activated carbon · Wood wastes · Northern hardwood pins-fines · Wood dust · Vacuum pyrolysis · Vacuum gasification · CO_2

1 Introduction

Activated carbon (AC) is a highly porous carbonaceous structure which is mainly composed of carbon atoms [1]. AC has a complex network of internal pore structures and a large surface area, exhibiting variable surface chemistry characteristics due to its specific production process and

✉ Zhiyong Cai
zhiyong.cai@usda.gov

[1] Ligwood LLC, Madison, WI 53705, USA

[2] Forest Products Laboratory, USDA Forest Service, One Gifford Pinchot Drive, Madison, WI 53726-2398, USA

raw material source [1]. With tremendous oxygen-containing functional groups presenting on its surface which can serve as adsorption centers or active sites, AC demonstrates a high degree of reactivity to gaseous molecules and ionic adsorbates [2]. Carbon consists of 85–97% activated carbon [3], therefore, any economical material with a high carbon content can be used as a raw material resource to produce AC. In recent years, agricultural wastes have been investigated as precursors to produce ACs due to their high carbon content [4], availability and relatively low mineral content [5]. Schlesinger [6] reported that the carbon content of biomass is found to be approximately 45–50% (by dry mass). On a moisture-free and ash-free basis, most biomass contains ~ 80% volatile matter and 20% fixed carbon. Thus, biomass is generally more reactive than coal during the pyrolysis process making biomass more suitable to produce high-quality ACs. Activated carbon can be made from any biomass residues or agricultural wastes such as grass, wood, root, stem, bark, flower, leaf, fruit peel, rice husk, nutshell, and stone [7]. Approximately 100 billion metric tons of carbon are fixed by greeneries on Earth each year [8]. Biomass for AC production can be classified into woody and non-woody resources. Cellulose, hemicellulose, and lignin are three main compositions in woody products, whereas non-woody resources are composed of cellulose, hemicellulose, lignin, lipids, protein, sugar, hydrocarbon, and starch [9]. The ash in biomass feedstocks is composed of inorganic compounds containing mostly silicon, potassium, calcium, sodium, phosphorus, and chlorine. There are less mineral contents in woody resources (usually < 1%), but more ash components (up to 15%) in herbaceous biomass and agricultural residues [10]. A much higher portion of feedstocks, such as animal manures, result in ash often exceeding 20%. ACs are commercially manufactured from coconut shell, hard and softwood, peat, lignite coal, bituminous coal, olive pits and other carbonaceous materials [11]. Large amounts of wood wastes are produced in municipal solid waste (MSW), construction and demolition (C&D) debris, wood residues from wood processing industries (WPI), primary timber process (PTP), and the paper and pulp industry (PPI) [12]. Wood wastes generated from MSW and from C&D debris have been marketed to fuel and mulch [13]. C&D wood wastes are used to produce clean pulp chips usable for the PPI [12, 14]. Wood waste residues from WPI, PTP and PPI include bark, sawmill slabs, wood dust, wood pins/fines, sawdust, and peeler log cores [15]. Nearly all these residues are currently used to produce products, primarily, fiber for paper, building panels (particleboard, medium-density fiberboard, hardboard, and insulation board), landscape mulch, animal bedding, and/or fuel [16]. In past decades, much work has been done to valorize agricultural residues, especially wood waste, to value-added products such as composites [17], bio-oils [18], and carbon-based materials such as activated carbon [1], graphite [19], graphene [20], etc.

AC products are prepared through different technologies in the industry. Generally, production methods for ACs can be classified into two clearly defined groups [21]: physical activation and chemical activation [1] methods. Physical activation is the first commercial and widely used AC production process, and it consists of two consecutive stages: the raw feedstock is first thermal pyrolyzed at high temperature under an inert atmosphere, then followed by activation using gaseous oxidation agents (steam, CO_2, air, O_2, etc.). Pyrolysis/carbonization, where devolatilization of biomass takes place, is carried out at medium or high temperatures, to produce a char rich in carbon [22]. Another commercialized method for AC production is chemical activation, which involves the reactions of a carbon precursor with chemical reagents. In the chemical activation process, raw carbon precursors are directly impregnated with certain chemical agents such as H_3PO_4, H_2SO_4, HNO_3, $ZnCl_2$, NaOH and KOH. Occasionally H_2O_2, K_2CO_3, $CaCl_2$, and formamide are used at room temperature [23, 24]. Each activation reagent produces a very different pore development in the carbon precursor. During this step, the process variables are carefully controlled to obtain AC products with different pore structures for different end-uses. These important process variables include the chemical agent and precursor mass ratio, the impregnation agent, temperature, time and stirring rates [25]. The resulting precursor-agent mixture is later thermally treated at temperatures ranging from 500 to 800 °C under inert gases [1]. Significant levels of chemical reagents are first added to biomass feedstock in the chemical activation process; therefore, the operability of chemical activation processes is strongly dependent upon efficiently recovering the reagent for recycling. This involves a consequent leaching stage, followed by an additional operation consisting of drying the washed carbon. Compared to the two kilns that are normally employed for pyrolysis/carbonization and activation in industrial physical activation, chemical activation requires only a single kiln. The chemical activation method is generally used to produce powdered activated carbon from sawdust, wood or peat [1]. Activated carbon from the chemical activation process contains a considerable inorganic content, which may lead to environmental contamination [26] and reduced the adsorption capability of AC materials. Depending on the chemical reagents used, impurities like zinc (Zn), phosphorus (P), and sulfur (S) can be found in the AC product, which may also result in raising the operating cost due to the additional purification process [27]. The main advantage of physical activation is that it avoids the mixing of impurities derived from the chemical activating agent [26]. Therefore, physical activation is more

favorable than chemical activation concerning environmental safety since no chemical reagents are used.

Two consequential steps are performed in the physical activation process, i.e., pyrolysis and activation. Chars rich in carbon are first formed during the thermal pyrolysis steps. Based on reactions, the pyrolysis process can be divided into two regions: primary pyrolysis and secondary pyrolysis (Scheme 1). Primary pyrolysis occurs at relatively low temperatures within a general temperature range of 200–400 °C [28]. By heating biomass under an inert atmosphere, gases (CO_2, H_2O, CO, CH_4 and H_2), volatiles, tar, and char are the main products derived through primary reactions. With the increase of heating temperature and holding time, the products of primary pyrolysis including some volatiles and especially tar, experience further reactions (secondary reaction). Secondary pyrolysis reactions generally occur at temperatures above 500 °C for biomass tar. The secondary reactions include thermal cracking, re-condensation, re-polymerization, etc. During the secondary pyrolysis step, the pores formed in the primary char are enlarged. These pores offer many reaction sites where more secondary reactions take place, leading to more carbon deposits to the char matrix. Conversely, the volatiles generated from the inner char matrix must diffuse through the pores in the char and desorb from the outer char surface. At high temperature, these secondary reactions are kinetically fast and non-selective processes resulting in more and more carbon deposits on the pore walls, leading to the pores becoming smaller and narrower. Thus, the retention time of the tars increases, leading again to more carbon deposition. Carbon deposition in the pores can rapidly seal off the pores. Due to the restraint of the diffusion, a closed pore is undesired in chars and is a disadvantage for the further activation process [29].

Production of high surface area and porous activated carbons requires avoiding the formation of closed pores in chars during the pyrolysis process. Several strategies have been proposed to eliminate or reduce the formation of the closed porosity in chars. The first strategy is to concurrently feed in the activation gases (CO_2 and H_2O) with inert gases during the pyrolysis process. In this method, volatiles are reformed to CO and H_2 by CO_2 or H_2O at high temperature, which prevents the blocking of pore mouths by reducing the thermal cracking of tars [30]. Another method to reduce carbon deposition in the pores of the char is vacuum pyrolysis [31]. Volatiles diffuse rapidly out of the inner pores of char under vacuum pyrolysis leading to a much shorter residence time as compared to atmospheric carbonization. Therefore, secondary reactions of these volatiles in the pores of the char are limited, and deposited carbon in pores is decreased considerably. It was previously observed that wood char from vacuum pyrolysis is more reactive to CO_2 oxidation than those produced by atmospheric pyrolysis [32]. Char from vacuum pyrolysis demonstrates more open pores and is more easily activated by CO_2 and H_2O [33]. It was found that under the same activation conditions, vacuum pyrolytic charcoal yields an activated carbon with a higher specific surface area as compared to char from atmospheric pyrolysis [34]. It was found that charcoal from vacuum pyrolysis reacts faster with steam as compared to charcoal produced during atmospheric carbonization [35].

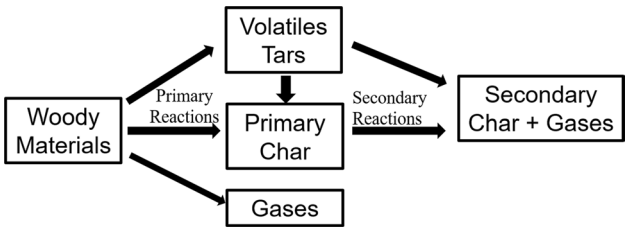

Scheme 1 Pyrolysis of woody materials and char formation

The objective of this present work is to study the possibility of preparing effectively activated carbons from wood waste through physical pyrolysis and CO_2 activation, vacuum pyrolysis and CO_2 activation, CO_2 gasification, and vacuum CO_2 gasification processes. The effects of different process conditions, such as the vacuum pyrolysis temperature, heating time, and heating rate on the surface area, the pore structures, and surface functional groups were examined using various techniques such as N_2 physisorption, thermogravimetric analysis (TGA), Fourier transform infrared spectroscopy (FTIR), and scanning electron microscopy (SEM).

2 Materials and methods

2.1 Materials

Northern hardwood wood dust and pins/fines (Fig. 1) from the paper and pulping process were provided by Domtar. The proximate moisture analysis was carried out following ASTM D4442-07 standard [36]. The moisture contents of these samples were 8.20 ± 0.25 wt%, and 7.1 ± 0.23 wt%, respectively (Table 1). The ash content of these samples was measured according to ASTM D1102 [37]. The ash content of wood dust and pins/fines were 1.10 ± 0.22 wt% and 1.26 ± 0.17 wt% respectively (Table 1). Elemental analysis of the wood dust and pins/fines was carried out on a PE 2400 CHNS Elemental Analyzer (PerkinElmer, Waltham, MA, USA). The oxygen content was calculated by the exclusion of C, H, and N. The main element contents (C, H, O, and N) are listed in Table 1.

Thermal degradation and stability of wood dust and pins/fines were evaluated by thermogravimetric analysis (TGA, PerkinElmer, Akron, OH, USA). TGA experiments were

performed at the temperature of 50 °C to 800 °C with a heating rate 5 °C/min under nitrogen atmosphere (20 mL/min), ~ 10 mg sample was used in each run.

2.2 Preparation of chars/activated carbon

2.2.1 Atmospheric pyrolysis (AP) and CO_2 activation

The pyrolysis and activation processes were performed on a home-built fixed bed tubular reactor system (2-in O.D., 316 stainless-steel) (Fig. 2) which was placed in an electrical furnace. A mechanical vacuum pump was connected to

Fig. 1 Photos of northern hardwood pins/fines and wood dust samples provided by Domtar

Table 1 Elemental analysis of northern hardwood wood dust and pins/fines based on dry matter (wt%)

Sample	C	H	O	N	Ash	Moisture
Pins/fines	49.91 ± 0.25	8.01 ± 0.31	40.75 ± 0.38	0.28 ± 0.07	1.10 ± 0.22	8.21 ± 0.25
Wood dust	49.82 ± 0.29	8.20 ± 0.19	39.11 ± 0.45	0.35 ± 0.08	1.26 ± 0.17	7.23 ± 0.31

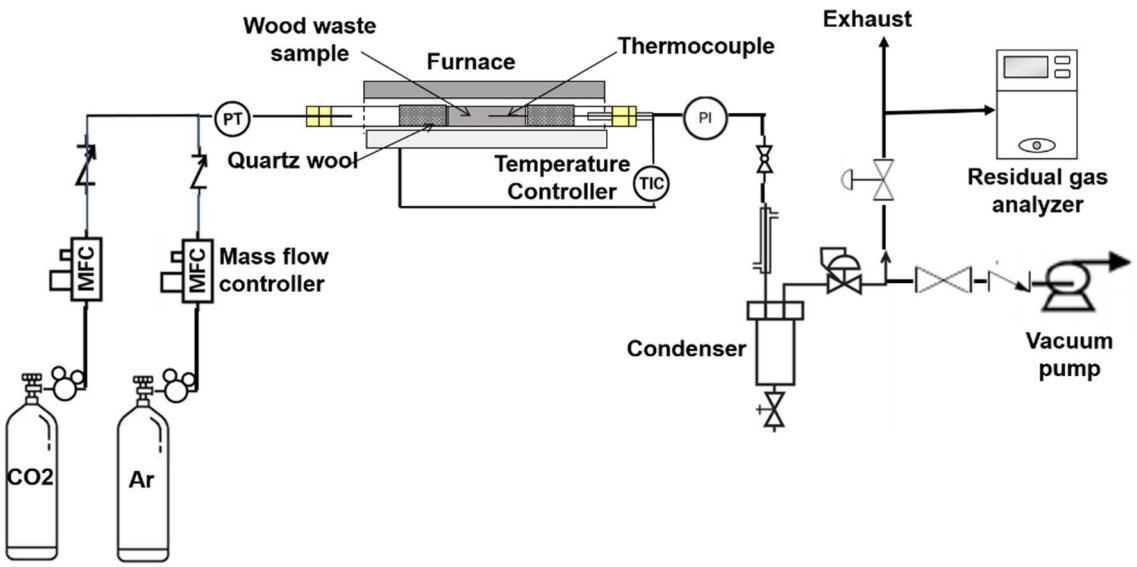

Fig. 2 Schematic of the experimental system

the outlet of the reactor system. The heating rate, pyrolysis temperature, and heating time were programmed using the control panel. For each pyrolysis run, 80 g of wood waste were packed in the middle of the tubular reactor. A thermocouple (type K) was inserted and fixed in the center of the sample bed to measure the sample temperature during the temperature-programmed pyrolysis process. An argon flow (99.99%) was first introduced into the reactor at a flow rate of 500 mL/min for 30 min. The reactor was heated at a rate of 10 °C/min to a pyrolysis temperature and kept at temperature for 60 min. An on-line Hiden QGA quantitative gas analysis system was used to monitor and analyze the gaseous products [38]. The signals from the mass spectra of 2, 15, 28, 44, and 78 (m/z) were identified as major contributors from the evolved gases and volatiles like H_2, CH_4, CO, CO_2, and benzene, respectively. Pyrolysis of the wood waste samples was accomplished at five temperatures (400 °C, 500 °C, 600 °C, 700 °C, and 800 °C). The produced chars from the pyrolysis process were either taken out of the reactor and denoted as Char-AP samples or further activated into AC samples. The activation process was performed in the same reactor system. For the activation experiments, the activation temperature was selected as 800 °C. The reactor was heated from room temperature to the activation temperature and held for 60 min. Argon (100 mL/min) and CO_2 (400 mL/min) were co-fed into the reactor during the activation process. The products prepared through the activation process are referred to as AC-AP-CO_2 (activated carbon) samples. The yield of chars and ACs was calculated by the equation of

$$X\% = \left(\frac{A}{B}\right) \times 100\%$$

where A is the mass of the solid carbon residue after heating, and B is the mass of raw feedstock before heating.

2.2.2 Vacuum pyrolysis (VP) and CO_2 activation

The vacuum pyrolysis process was carried out in the same reaction system as atmospheric pyrolysis (Fig. 2). For each vacuum pyrolysis run, 80 g of wood waste was placed in the reactor. The air in the reactor was evacuated by the vacuum pump before the pyrolysis process and steady pressure of about 0.5 atm vacuum was attained by flowing 500 mL/min argon. The reactor was heated at a specific rate from room temperature to a selected pyrolysis temperature and held for 60 min. After pyrolysis, the reactor was naturally cooled down to room temperature while kept in the same vacuum. The produced chars from the vacuum pyrolysis process were either removed from the reactor and denoted as Char-VP samples or further activated using CO_2 at 800 °C for 60 min. The chars from the vacuum pyrolysis were then activated by CO_2 to prepare the final activated carbons. For the activation process, the activation temperature selected was 800 °C. During the CO_2 activation process, argon (100 mL/min) and CO_2 (400 mL/min) were co-fed into the reactor. The activated carbons prepared in this process are referred to as AC-VP-CO_2 samples.

2.2.3 Atmospheric CO_2 gasification (AG-CO_2)

The CO_2 gasification process was performed on the same system as the atmospheric pyrolysis process. For each CO_2 gasification run, 80 g of wood waste was packed in the middle of the tubular reactor. Argon (100 mL/min) and CO_2 (400 mL/min) were first introduced into the reactor for 30 min. The reactor was then heated at a rate of 10 °C / min to a gasification temperature and kept at temperature for 60 min. After gasification, the furnace was cooled down to room temperature while under the Ar/CO_2 atmosphere. The chars from the CO_2 gasification process were denoted as Char-AG samples.

2.2.4 Vacuum CO_2 gasification (VG-CO_2)

The vacuum CO_2 gasification (VG-CO_2) process was carried out in the same reaction system as atmospheric pyrolysis (Fig. 2). For each VG-CO_2 run, 80 g of wood waste was placed in the reactor. The air in the reactor was evacuated by the vacuum pump before the pyrolysis process and a steady pressure of about 0.5 atm vacuum was attained by flowing 100 mL/min argon and 400 mL/min CO_2. The sample in the reactor was vacuum gasified with flowing CO_2 at a heating rate of 10 °C/min to a final temperature and kept at the temperature for 60 min. After VG-CO_2. The resulting chars from the VG-CO_2 process were denoted as Char-VG-CO_2 samples.

2.3 Characterization of the prepared activated carbons

The specific surface area and pore structure characteristics of the prepared chars and activated carbons were measured by nitrogen adsorption over a surface area analyzer (Tristar II, Micromeritics, USA). The sample was degassed under a vacuum at 300 °C for 3 h before measurement. The specific surface area (S_{BET}) of prepared chars and AC samples were measured by N_2 physisorption and calculated using the Brunauer–Emmett–Teller (BET) method. Elemental analyses of solid chars and ACs were performed using a CHNS/O analyzer (Perkin Elmer PE2400 series II, PerkinElmer, Billerica, MA, USA). The ATR-FTIR spectra of wood wastes, wood char, and activated carbon samples were recorded with a ATR-FTIR spectrometer (Thermo Scientific, Nicolet iZ10,Thermo Fisher, Waltham, MA, USA) at a resolution of 4 cm^{-1} for 64 scans in 500–4000 cm^{-1} range. The

morphology of solid products was investigated using a scanning electron microscope (SEM) operated with accelerating voltage of 3 kV, all samples were plasma coated with 10 nm Pt before being transferred into the vacuum chamber.

3 Results and discussion

3.1 Thermogravimetric analysis (TGA)

Figure 3 shows mass loss curves and derivative thermogravimetry (DTG) curves for northern hardwood pins-fines (Fig. 3a) and wood dust samples (Fig. 3b). The results show a scheme of pyrolysis in the pins-fines sample that is clearly different from wood dust. With respect to the pins-fines sample, significant mass loss was observed between 180 and 550 °C, and two major peaks were present at 329.8 and 403.7 °C and one shoulder between 180 and 300 °C. The mass loss shoulder is ascribable to hemicelluloses and the amorphous fraction of cellulose [39]. The first major mass loss peak at 329.8 °C could be attributed to the decomposition of crystalline cellulose (ranging between 200 and 370 °C). The second major mass loss peak could be related to the decomposition of lignin and related compounds containing phenol structures (ranging between 370 and 530 °C) [40]. Pyrolysis reactions occur in this zone (ranging between 180 and 550 °C), and a primary wood char is obtained. The carbonization process is ongoing with increasing temperature from 550 to 800 °C. After the primary pyrolysis step, mass loss is very little during the carbonization process.

Figure 3b shows TGA/DTG curves obtained in the wood dust sample. In the wood dust scheme, pyrolysis shown in the DTG curve presents a single major mass loss at 329.8 °C and one shoulder at 326.6 °C in the temperature range of 170–500 °C. The shoulder mass loss is essentially pronounced for hemicellulose and amorphous cellulose decomposition. The only strong mass loss peak is mainly contributed by the hemicellulose and cellulose decomposition [41]. There should be small amounts of lignin in the wood dust sample and decomposition of lignin might be overlapped by the sharp cellulose peak since decomposition of lignin usually goes through a wide temperature range [42]. Figure 3b demonstrates that the wood dust sample is mainly composed of cellulose and hemicellulose components while the composition of the pins-fines sample is more similar to the whole wood samples [43].

3.2 Fourier transform infrared spectroscopy (FTIR)

Cellulose, hemicelluloses and lignin in woody resources demonstrate different characteristics and specific FTIR absorptions. Figure 4 shows the infrared spectra recorded for the northern hardwood pins/fines: raw pins-fines, thermally treated by VP at 500 °C, thermal treated by VP at 800 °C, and activated by CO_2 at 800 °C. Figure 4a shows the FTIR spectra of wood waste (northern hardwood pins/fines) in the ranges of 3800–2500 cm^{-1}. The first band (3700–3000 cm^{-1}) corresponds to the hydroxyl groups adsorbed by the wood (especially the hemicellulose and lignin molecules) and the bands at 2800–2980 cm^{-1} correspond to asymmetric -CH_3 and symmetric -CH_2. Figure 4b illustrates the FTIR spectra of wood waste (northern hardwood pins/fines) in the ranges of 1800 to 800 cm^{-1}. A strong band is found at 1732 cm^{-1} that can be associated with unconjugated C=O in unconjugated ketone, carboxyl, and ester groups. A shoulder absorption peak at 1650 cm^{-1} is related to ring conjugated C=O stretch. Bands located at around 1595, 1505, and 1420 cm^{-1} were assigned to vibrations of aromatic rings [41, 42]. The bands at 1456, 1368 and 1325 cm^{-1} are related to aliphatic (–CH-), (–CH_2) and (–CH_3) deformation. The peaks at 1266 and 1234 cm^{-1} were assigned to the aryl breathing with C=O stretch, and C–C, C–O, and C=O stretches, respectively [44, 45]. The band in 1156 cm^{-1} was assigned to aromatic C-H in plane deformation. The band

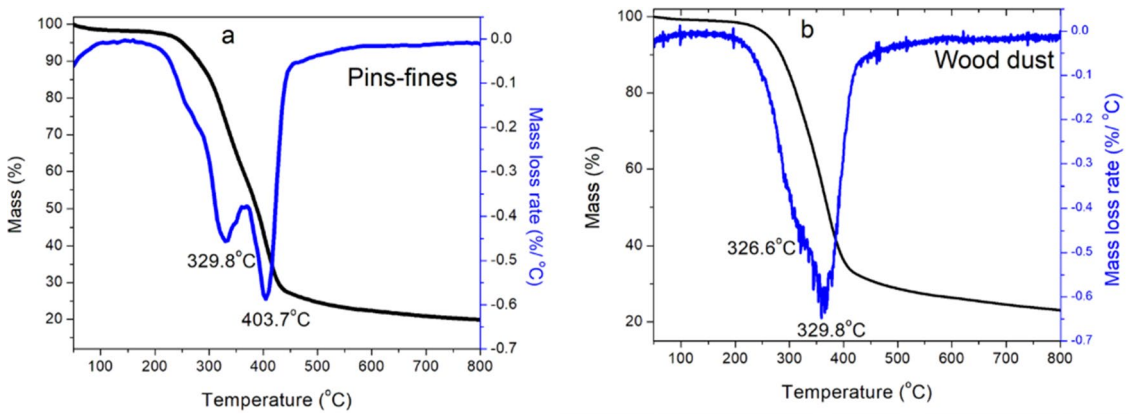

Fig. 3 Typical TGA and DTG of wood wastes: northern hardwood pins-fines (**a**) and wood dust (**b**)

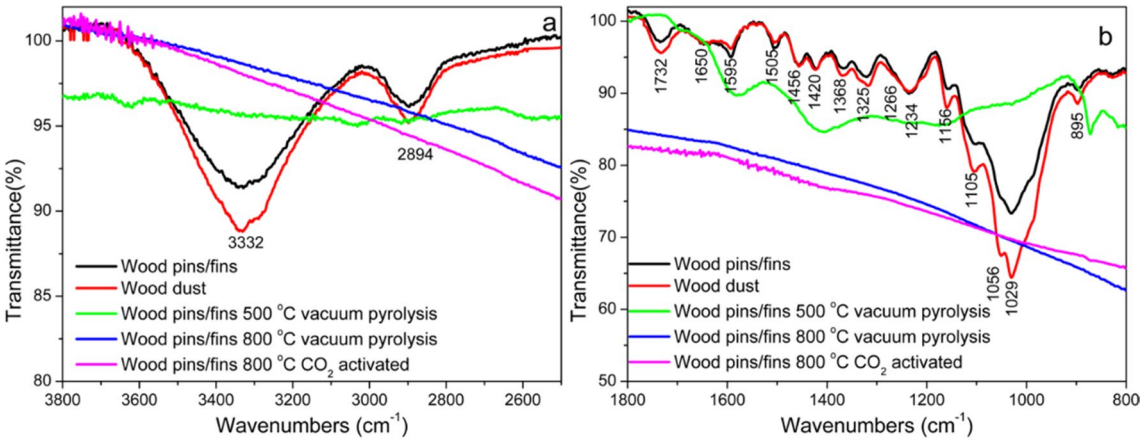

Fig. 4 Typical FTIR spectrum of wood waste (northern hardwood pins/fines) in the ranges of 3800–2500 cm^{-1} (**a**) and 1800–800 cm^{-1} (**b**)

at 1105 cm^{-1} was contributed to the vibration of C-O and O–H. The peaks at 1056 and 1029 cm^{-1} were contributed by aliphatic ether C–O–C and alcohol C–O stretching in secondary alcohol [46]. The band at 895 cm^{-1} was assigned to the deformation vibrations of C–H bonds in the aromatic rings [47]. The band at 815 cm^{-1} was generated by the out of plane vibrations of aromatic C–H [48]. Both the northern hardwood pins/fines and wood dust samples demonstrate typical FTIR absorption peaks of cellulose [49], and the wood dust shows stronger absorption bands of cellulose, this means more cellulose and hemicellulose contents in the wood dust sample, it is in agreement with the TGA results (Fig. 3b). After thermal treatment by VP at 500 °C, the bands detected were 1595, 1420, and 863 cm^{-1} which were attributed to the deformation of (C=C) the aromatic cycle of lignin, scissoring (CH_2 and CH_3) of lignin, and the deformation vibrations of C-H bonds, respectively. The bands due to C=O, C–O, aliphatic C–O = C, and –OH represent oxygenated functional groups of cellulose and lignin and are mostly eliminated after heating at 500 °C in vacuum condition for 60 min. The FTIR spectra of thermally decomposed wood pins-fines samples demonstrate that almost all the functional groups existing in wood have disappeared after going through the thermal decomposition at 800 °C.

3.3 Main gaseous products during different thermal treatment processes

Figure 5 shows the typical gas profiles of H_2, CH_4, CO and CO_2 evolved from northern hardwood pins-fines under three different thermal treatment processes. The temperature was increased to 800 °C by 20 °C/min and kept for 60 min. Table 2 summarizes the evolution temperature ranges, peak temperatures and the maximum formation rate of four main gaseous products.

Hydrogen presented in wood is mainly as C–H in aliphatic CH_x ($x = 1$, 2, or 3) and aromatic rings. The carbon–hydrogen bond (C–H) is very stable, the dissociation energy to break apart C–H [49] is over 350 kJ/mole, therefore, it can only be broken down when the heating temperature is high enough (> 700 °C) [40]. The hydrogen formation under the AP process (Fig. 5a) demonstrates two peaks: a shoulder peak at 615.4 °C and a very sharp peak at 781.1 °C. The hydrogen generation rate at the two peaks are 3.73 and 7.04 mL/min g (wood waste) respectively. The low-temperature hydrogen creating peak could be attributed to the secondary pyrolysis reaction and the decomposition of C–H in cellulose and hemicellulose, while the high-temperature hydrogen peak is contributed by the thermal cracking of C–H in aliphatic CH*x* ($x = 1$, 2, or 3) and aromatic rings in lignin [40]. The H_2 evolution profile of wood pins-fines during AG was similar to that of the AP process (Fig. 5b). However, H_2 formation was promoted in the presence of CO_2 since CO_2 is a strong oxidation agent at high temperature. Both hydrogen peaks were shifted to lower temperatures of 547.2 °C and 751.9 °C, respectively, but the hydrogen formation rates were reduced to 1.18 and 5.35 mL/min g because of the reverse water–gas shift reaction (RWGSR) ($CO_2 + H_2 = CO + H_2O$) [39]. In this reaction, the hydrogen from the thermal dissociation of C–H in aliphatic chains and aromatic rings in cellulose and lignin was consumed through RWGSR. The H_2 evolution curve during AP-CO_2 is dramatically different from those during the AP and AG processes (Fig. 5c). Only a trace amount of H_2 (0.11 mL/min g) was produced at 800 °C since most of the hydrogen was released under AP treatment.

Three CH_4 evolution peaks at 488.9, 560.3 and 766.1 °C were observed during the thermal decomposition of wood pins-fines by AP process (Fig. 5a). The maximum methane formation rates were 2.07, 2.25, and 0.80 mL/min g, respectively. The first two peaks with higher formation rates were

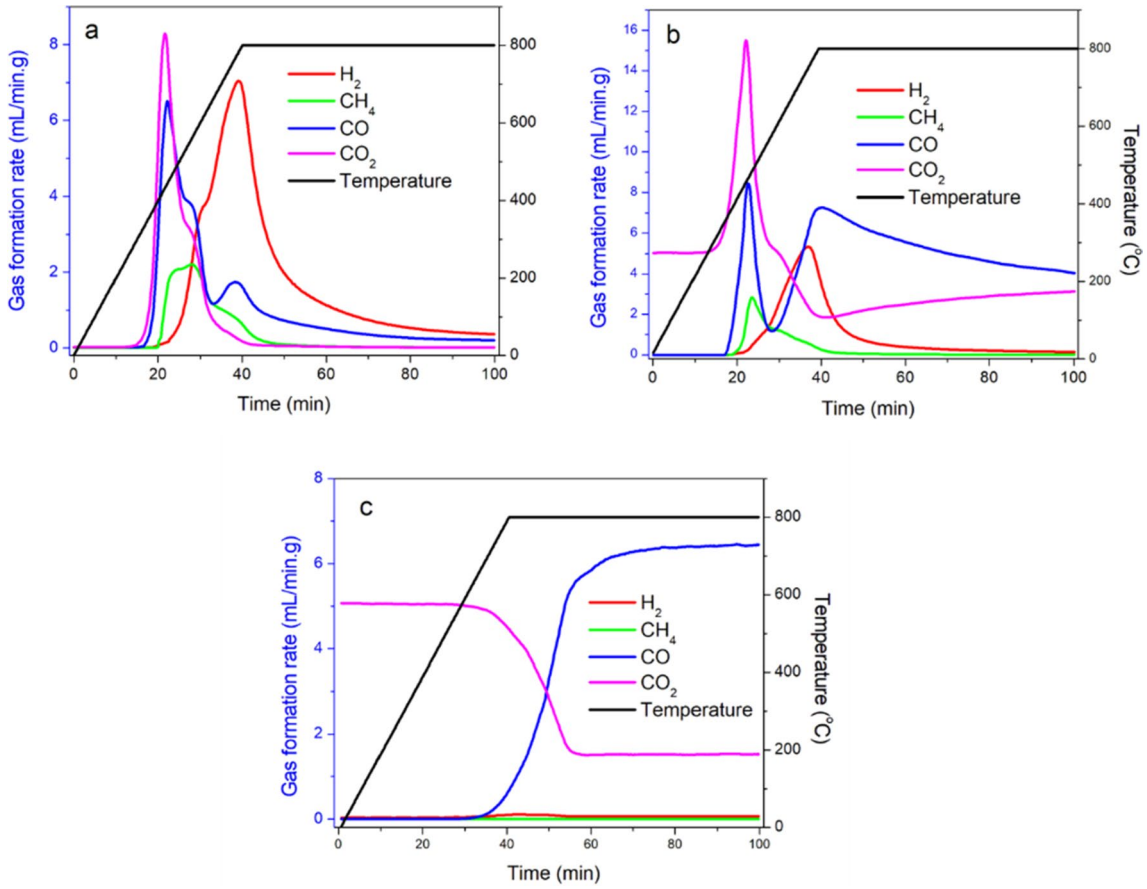

Fig. 5 Evolution of gas products from wood pins-fines under different thermal treatment processes by increasing to 800 °C with a heating rate of 20 °C/min and kept for 60 min: **a** atmospheric pyrolysis under argon (AP), **b** atmospheric CO_2 gasification (AG), and **c** CO_2 activation after AP at 800 °C (AP-CO_2)

Table 2 Summary of gas evolution time, peak temperatures and peak generation rate of wood pins-fines under different thermal treatment processes by increasing to 800 °C with a heating rate of 20 °C/min and kept for 60 min: atmospheric pyrolysis under argon (AP), atmospheric CO_2 gasification (AG), and CO_2 activation after AP at 800 °C

Gas	Thermal treatment processes		
	AP	AG	AP-CO_2
	Time (min), Peak temperature, °C (peak generation rate, mL/min g)		
H_2	31.1, 615.4 (3.73) 39.1, 781.1 (7.04)	26.7, 547.2 (1.18) 36.9, 751.9 (5.35)	46.6, 800 (0.11)
CH_4	24.4, 488.9 (2.07) 28.0, 560.3 (2.25) 38.4, 766.1 (0.80)	23.6, 485.5, (2.83) 28.0, 569.5 (1.53)	–
CO	22.2, 443.7 (6.52) 27.8, 557.0 (3.79) 38.2, 764.8 (1.74)	22.5, 465.2 (8.45) 39.9, 800 (7.26) 688–1000 (745)	33.2, 687.0 (0.06) 57.6, 800 (5.69)
CO_2	21.7, 433.6 (8.29) 26.6, 531.2 (3.30)	22.1, 455 (10.51) 26.7, 531.5 (1.63) 41.0, 800 (3.15)[a]	33.2, 687.0 (0.05)[a] 57.6, 800 (3.48)[a]

[a]Means values in parentheses are gas consumption

mainly caused by the breaking of weakly bonded methoxy groups (O-CH_3) [40, 51, 52] in cellulose and lignin and the fragmentation of side aliphatic chains [47, 50]. The evolution of CH_4 at high temperatures was attributed to the secondary pyrolysis of cellulose and aromatic volatile intermediates [40, 53] and the rearrangement of the skeleton of cellulose and lignin structures [40, 51–53]. The CH_4 evolution profile during AG process was different from that of AP process,

the main evolution peak shifted to a lower temperature of 485.5 °C with the generation rate of 2.83 mL/min g. This indicated that the presence of carbon dioxide accelerated the cracking of lignin methoxy [40] and aliphatic groups. In addition, the disappearance of the high-temperature CH_4 evolution peak suggested that the secondary pyrolysis of volatiles in the wood char matrix was suppressed by the existence of CO_2. Volatile intermediates adsorbed in micropores in char were gasified to CO, H_2O and H_2 products [30, 40]. No CH_4 formation was detected during AP-CO_2 process because of the AP treatment.

Three CO evolution peaks were observed during AP, at 443.7, 557.0 and 764.8 °C, respectively (Fig. 5a). The maximum CO evolution rates were 6.52, 3.79, and 1.74 mL/min g, respectively. The lower temperature CO evolution peak of 443.7 °C was due to the rupture of weakly bonded ether bridges and the decomposition of carbonyl groups [40, 54]. The CO evolution peak 557.0 °C was mainly because of the cleavage of aromatic bonded oxygens (i.e. methoxy and phenolic groups). The higher temperature CO formation at 764.8 °C was assigned to the secondary cracking of oxygenate volatiles and tars. Wood pins-fines gasification under atmospheric CO_2 (AG) showed two CO evolution peaks (Fig. 5b) at 465.2 and 800 °C with the formation rates of 8.45 and 7.26 mL/min g respectively. The first CO formation peak was assigned to the decomposition of ether, carbonyl, methoxy, and phenolic groups. The CO peak at 800 °C had a strong evolution trend, indicating that most of the oxygenate volatiles, tars, and part of the wood char residue was consumed by the gasification reactions ($Cs+CO_2 \rightleftharpoons 2CO$) to produce CO during the AG process.

CO_2 exhibited two evolution peaks (Fig. 5a, and Table 2) during the AP process. CO_2 mainly originated from the thermal decomposition of carboxyl (-COO^-) and ester (-CO–O-R) groups [41]. The CO_2 generation peak at lower temperatures (centered at 433.6 °C, the generation rate of 8.29 mL/min g) was because of decarboxylation reactions, while the cleavage of ester groups was predominantly responsible for the CO_2 evolution at 531.2 °C with a formation rate of 3.3 mL/min g. The evolution of CO_2 was significantly promoted under the CO_2 gasification (AG) process compared to that under AP, i.e., only one CO_2 formation peak appeared at 456 °C with a high generation rate of 10.51 mL/min g. CO_2 was observed to be consumed from 550 °C during the AG process (Fig. 5b). At low temperatures (550–600 °C), CO_2 might be consumed by active volatiles, tar and solid residues to form various acids and ketones as previously reported [42], while the consumption of CO_2 at high temperatures (600–800 °C) was because of the gasification reaction ($C+CO_2 \rightarrow 2CO$) along with CO releasing (Fig. 5b). During the AP-CO_2 process (Fig. 5c), CO_2 began to be consumed from 687 °C and reached a steady consumption rate of 3.5 mL/min g at 800 °C. Char-AP demonstrates a higher CO2 consumption temperature, indicating that Char-AP has a relatively lower gasification activity compared to the direct gasification of wood pins-fines. The evolution of gas products from the wood dust sample under different thermal treatment processes was also analyzed and the similar results were observed (the results were not presented here).

3.4 Yield of chars and activated carbons

Figure 6 displays the yield of the prepared chars and activated carbons from northern hardwood pins-fines at different activation temperatures (400 °C, 500 °C, 600 °C, 700 °C, and 800 °C) through different thermal treatment processes, the heating rate and holding time of the thermal processes were 20 °C/min and 60 min, respectively. The yield of the chars and ACs are decreasing with the increase of the pyrolysis/gasification/activation temperature. From Fig. 6, it is observed that the char yield was in the range of 34.5–20.0% at pyrolysis temperature between 400 and 800 °C by atmospheric pyrolysis (AP). The char yield decreased from 33.9 to 16.5% by the atmospheric CO_2 gasification (AG-CO_2). The yield of the chars from the vacuum pyrolysis (VP) is between 18.9% and 33.3%. The yield of Char-VG-CO_2 is in the range of 32.7–14.9%. The yield of AC-AP-CO_2 and AC-VP-CO_2 are in the ranges of 24.8–15.8% and 23.2–15.5%, respectively. The yield of the prepared chars and activated carbons from northern hardwood wood dust under different thermal treatment processes were also investigated and similar yield trends were obtained.

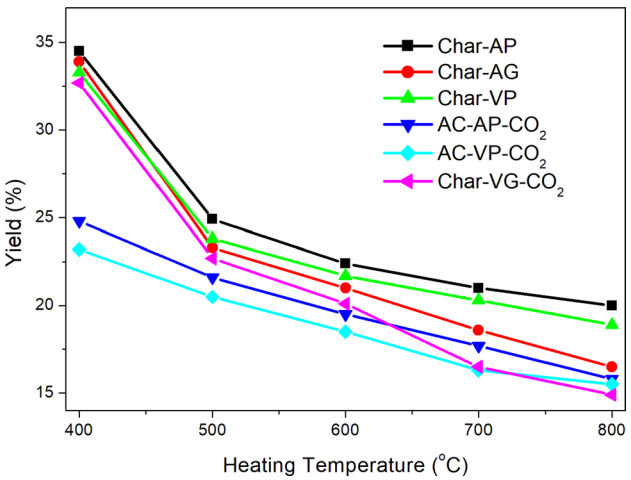

Fig. 6 Effect of heating temperature on the yields of char and activated carbon from wood pins-fines with different thermal treatment processes: atmospheric pyrolysis under argon (AP), atmospheric CO_2 gasification (AG), vacuum pyrolysis (VP), CO_2 activation after AP, CO_2 activation after VP, and vacuum CO_2 gasification (VG). The heating rate and holding time of the thermal processes were 20 °C/min and 60 min, respectively

Effect of heating temperature on the surface area (Fig. 7a) and the pore structure (Fig. 7b) of chars and activated carbons from wood pins-fines with different thermal treatment processes are profiled in Fig. 7. The heating rate and holding time of the thermal processes were 20 °C/min and 60 min. Figure 7a shows the effect of heating temperature on the surface area of chars and activated carbons. With increasing pyrolysis/activation temperature from 400 to 800 °C, the BET surface areas of Char-AP samples are relatively low for all the processing temperatures; they increase from 5.6 m^2/g of Char-AP-400 °C to 15.3 m^2/g of Char-AP-800 °C. BET surface areas of active carbon samples from AP-CO_2 and VP-CO_2 processes are higher than those from other processes, and they do not change much with the increase of activation temperature. The surface area of the ACs from AP-CO_2 decreased from 586.2 m^2/g at 400 °C to 515.8 m^2/g at 800 °C, CO_2 is an etching agent, the micro/meso-pores will be enlarged/etched by CO_2 at high temperature, parts of the pore structure will be collapsed/destroyed by CO_2 at a higher temperature which leads a decreased surface area; the surface area of the ACs from VP-CO_2 increased from 705 m^2/g at 400 °C to 769 m^2/g at 600 °C, then decreased to 745 m^2/g at 800 °C. The surface area of Char-VP samples increased from 25.9 m^2/g at 400 °C to 228.3 m^2/g at 800 °C. BET surface areas of Char-AG and Char-VG-CO_2 increase rapidly with increasing gasification/pyrolysis temperature. The surface area of the Char-AG increased from 7.5 m^2/g at 400 °C to 678.2 m^2/g at 800 °C. The surface area of the Char-VG-CO_2 increased from 78.0 m^2/g at 400 °C to 786.1 m^2/g at 700 °C, then further increased to 855.3 m^2/g at 800 °C. Char-VG-CO_2 samples exhibit higher surface area compared to those of other processes.

As previously discussed, the pyrolysis of biomass includes two main steps: primary and secondary pyrolysis. In primary pyrolysis, the biomass degrades into volatile gases, tar and char. The primary pyrolysis products are non-condensable (light) gases (e.g., CO, CO_2, H_2O, and H_2), light hydrocarbons (e.g., CH_4, C_2H_4), condensable gases and tars, solid residue (char), and mineral ash. If the products of primary pyrolysis undergo further reactions at higher temperatures and longer reaction times, secondary pyrolysis will dominate the reaction system. Secondary pyrolysis is a very complex process, a series of reactions occurred including cracking, polymerization, condensation, and carbon deposition [55]. These reactions can occur in the gas phase, at the char surface, or in the inner pores of the char. Significant condensable volatiles and tar in the primary pyrolysis are trapped in char micropores due to the diffusion limitation. These volatiles and tar will be cracking and thermally decomposing to carbon and hydrogen. Carbon atoms deposit on the micropore wall, while hydrogen atoms recombine into hydrogen molecules. With more volatiles cracking and the pores becoming smaller and smaller, the retention time of the tars increases. The increased retention time of tars results in more cracking and carbon deposition, while the greater retention time of the volatiles leads to a higher level of secondary reactions and increase the yield of solid char. Carbon deposition in the pores will lead to complete filling or blockage of the micropores which will significantly decrease the surface area of the char. This pore blockage can explain why the surface areas of the Char-AP samples are smaller, while the pore volumes and average pore diameters are larger than those produced from other processes: surface area of the Char-AP sample is mainly contributed by the macropores since the sample is lacking micropores.

Deposited carbon from the secondary pyrolysis will impact the further activation of the char. Due to the restraint of the diffusion, activation reagents like CO_2 and water molecules are limited to diffusion into micropores of the char and an extended activation time and a

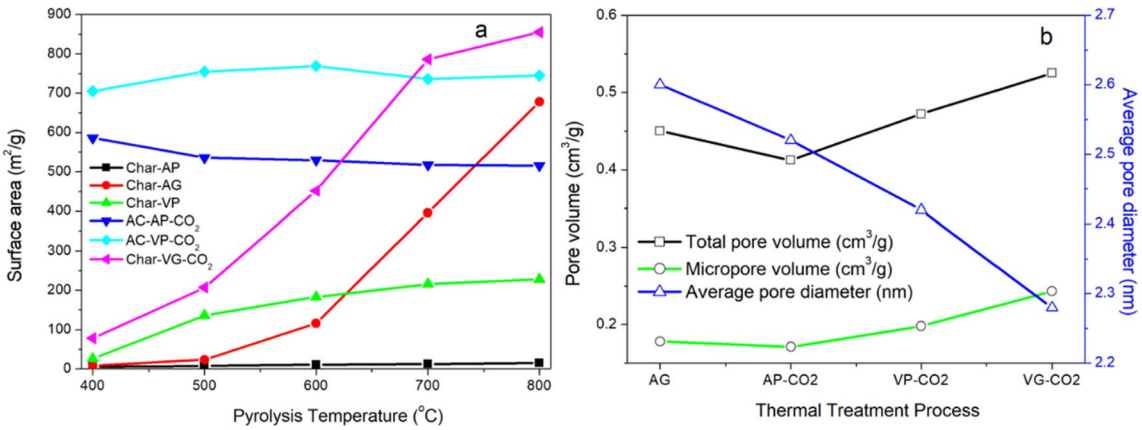

Fig. 7 Effect of heating temperature (400–800 °C) on the surface area of chars and activated carbons from wood pins-fines with different thermal treatment processes (**a**) and the pore structure of chars and activated carbons produced at 800 °C from different processes (**b**). The heating rate and holding time of the thermal processes were 20 °C/min and 60 min, respectively

higher activation temperature are needed in the second step. There are a couple of strategies to reduce or eliminate secondary pyrolysis. The first strategy is to run the pyrolysis under vacuum condition so condensable volatiles and tar will be removed from the micropores of the char before the carbonization process. The residence time is considerably shorter during vacuum pyrolysis, as compared to atmospheric pyrolysis. Therefore, the secondary pyrolysis reactions of the volatiles and tar, such as the formation of carbonaceous deposits on the surface and in the pores of the char, are limited under vacuum conditions [32, 33]. Char from vacuum pyrolysis has, therefore, a more "open" pore structure and is more easily activated than char from atmospheric pyrolysis. The second strategy is to perform the pyrolysis under a reactive atmosphere, such as CO_2, steam or air. The volatiles and tar will be gasified before the secondary pyrolysis reactions occur. As a result, carbon deposits on the surface and in the pores of the char are also limited [32, 33].

3.5 Effects of process conditions on AC yield, surface area and micropore structures

Figure 8 compares the yield, surface area, and micropore volume of the chars produced from northern hardwood pins-fines and wood dust by the VG-CO_2 process. The wood pins-fines shows higher yield than that of wood dust, but the chars from wood dust have higher surface areas and micropore volumes. From the TGA and FTIR results (Figs. 3 and 4), the wood dust may contain more cellulose and less lignin in the sample, which means less volatiles/tars (volatiles and tars are mainly polycyclic aromatic hydrocarbons from lignin) are generated from the wood dust samples during the primary pyrolysis step which leads to less secondary pyrolysis reactions, and less carbon deposition, therefore, the lower yield of the char from wood dust and higher surface areas and micropore volumes.

Gases, liquid (tars, condensable vapors, etc.), and solid (char) are produced during the pyrolysis of biomass [56]. The pyrolysis conditions, such as temperature and/or heating rate, and heating time are key factors that affect the

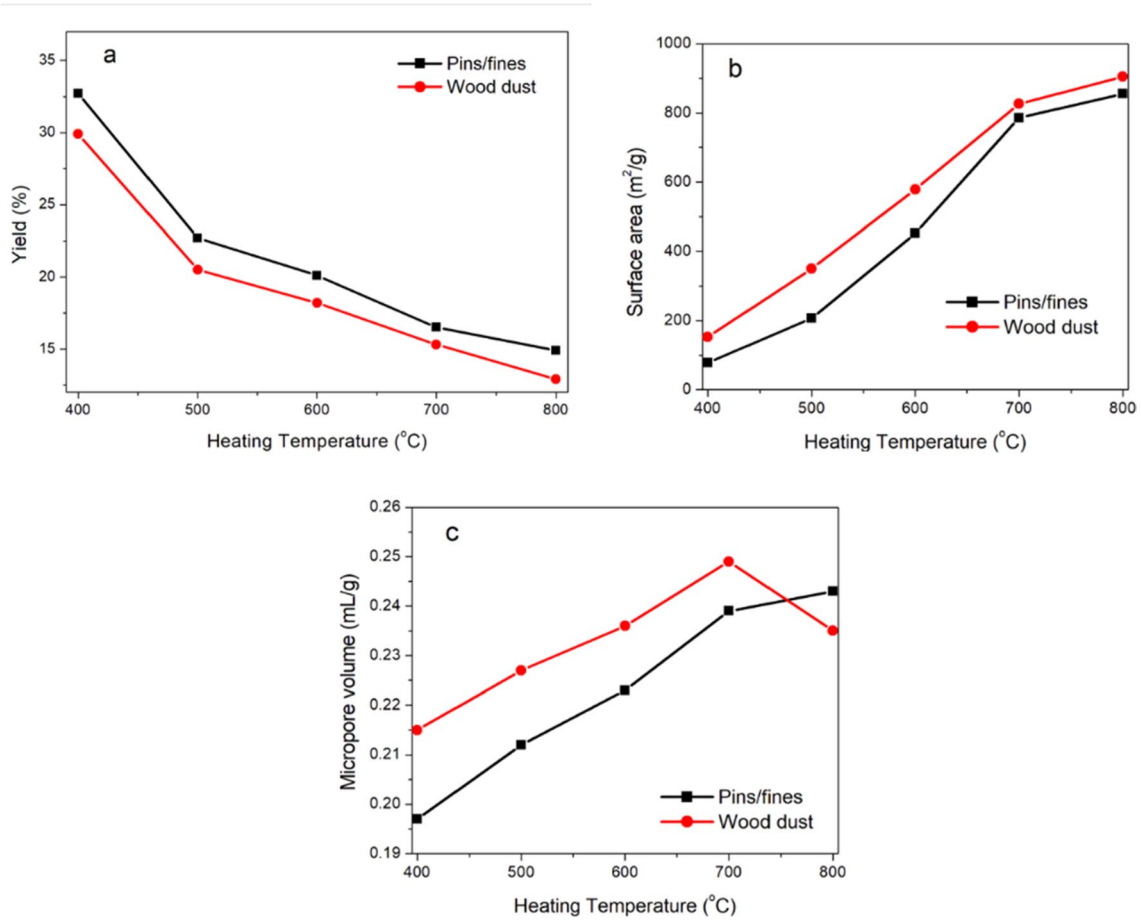

Fig. 8 The yield (**a**), surface area (**b**), and micropore volume (**c**) of the chars produced from northern hardwood pins-fines and wood dust through the VG-CO_2 process at 800 °C (heating rate, 20 °C/min, heating time, 60 min)

distribution among the three product fractions. High yields on liquid and/or gas, and low yield solid char are obtained when thermal treatment biomass with a fast-heating rate at high temperature [56]. To determine the effect of gasification temperature on the char properties, the wood pins-fines were vacuum gasified by CO_2 at 400 °C, 500 °C, 600 °C, 700 °C, 800 °C and 900 °C. Figure 9 shows the effect of heating temperature on the surface area and pore volume of the Char-VG-CO_2 samples. The surface area of the chars increased from 78.0 ± 5.5 m^2/g at 400 °C to 855 ± 18.2 m^2/g at 800 °C, and then decreased to 807 ± 15.7 m^2/g at 900 °C. The pore volumes of the chars increased from 0.197 ± 0.021 mL/g at 400 °C to 0.243 ± 0.026 mL/g at 800 °C, and then decreased to 0.209 ± 0.020 mL/g at 900 °C.

The effects of heating rate on the surface area and pore volume are shown in Fig. 10. The vacuum CO_2 gasification was performed at 800 °C for 2 h. Both the BET surface area and pore volume increase with increasing pyrolysis heating rate up to 20 °C/min, thereafter these values decrease with further increases in the heating rate up to 40 °C/min.

During the pyrolysis process, cellulose, hemicellulose, and lignin in the wood are first dehydrated to more stable intermediates anhydrocellulose and highly cross-linked lignin at low temperatures [57]. More anhydrocellulose and highly cross-linked lignin are produced in a slow heating rate process which benefits a high yield of char. During the fast heating process, the dehydration reaction is limited due to the short resident time at low temperature, less water is eliminated at low temperatures; hence, more organic volatiles will be gasified by steam at high temperature in the wood, and less secondary pyrolysis reactions occur in the pores and surface of the char [58]. The fast heating process will help the development of meso- and macropore structures during the subsequent activation as the CO_2 molecules can diffuse into the pores more easily. Consequently, the BET surface area and micropore volume decrease for the

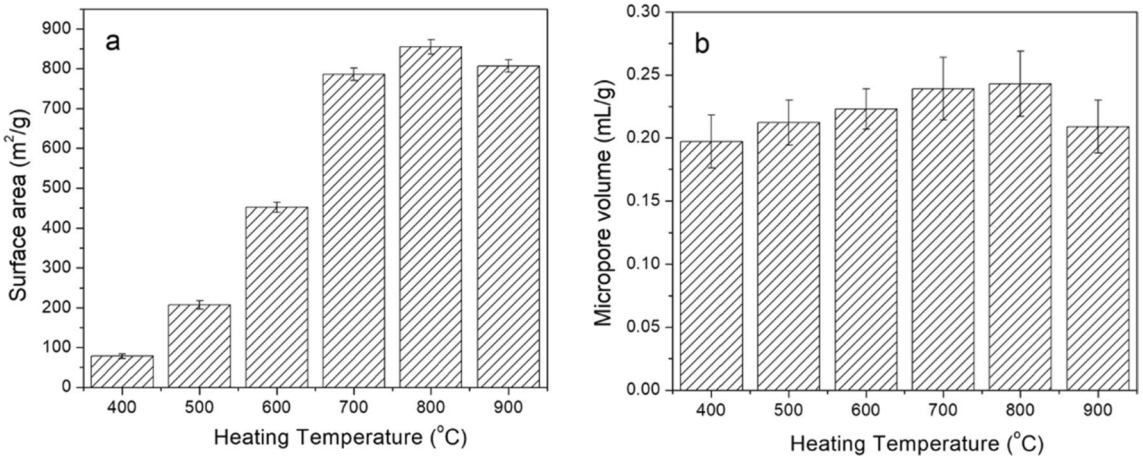

Fig. 9 Effect of gasification temperature on surface area and micropore volume of char from vacuum CO_2 gasification of wood pins-fines (heating rate, 20 °C/min, heating time, 60 min)

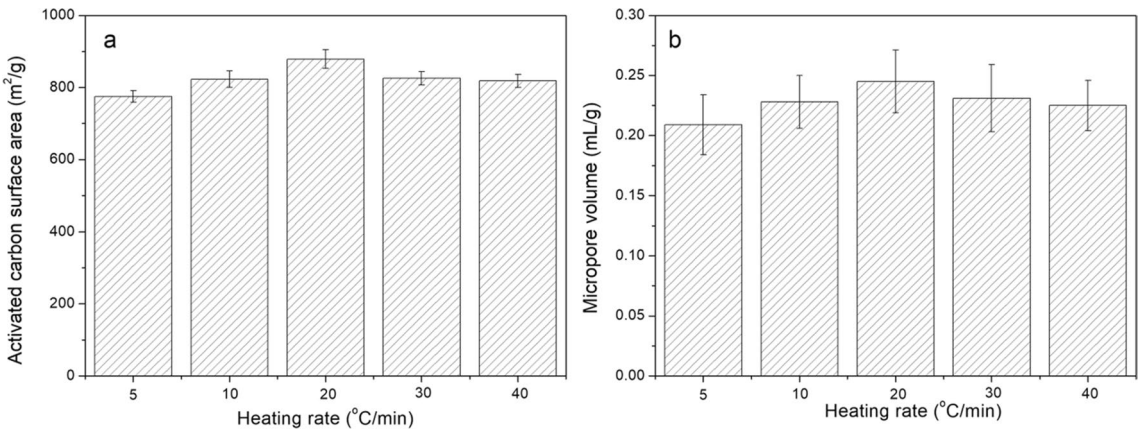

Fig. 10 Effect of heating rate on surface area and micropore volume of char from vacuum CO_2 gasification of wood pins-fines at 800 °C for 2 h

heating rates greater than 20 °C/min. The activated carbon with the highest BET surface area of 878.8 ± 25.6 m^2/g and micropore volume of 0.247 ± 0.023 mL/g was obtained from the char pyrolyzed at 20 °C/min.

The effect of gasification heating time on the surface area and pore volume of the chars from VG-CO_2 process at 800 °C is shown in Fig. 11. The surface area and pore volume first increase with increasing hold time up to 2 h, before decline sets in. A significant increase of the BET surface (from 602 to 878.8 m^2/g) was observed from 0.5 to 2 h, and then decreased at 2.5 h to 825.2 m^2/g. The same effect occurs to the pore volume responses involved with a higher increase in micropores from 0.5 to 2 h (from 0.195 to 0.247 cm^3/g). Initially, increasing VG hold time resulted in increased release of volatile matter and gasification of volatiles and tar thereby forming increased primary pore structures within the chars. Subsequently, activation of these chars by CO_2 further improves the porosity and pore surface area. However, a prolonged heat treatment at 800 °C will lead to increasing gasification and carbon structures in the chars which are etched, resulting in enlarged and collapsed pores and decreasing pore surface area with increasing heating time. The enlarging and collapsing of the micropores in chars correspond to decreasing pore surface area and micropore volume with increasing VG hold time.

3.6 Morphologies of char and AC samples

The morphology of chars/ACs produced at different pyrolysis/gasification conditions was characterized using SEM. The results of SEM analysis of the char by AP process are shown in Fig. 12a. SEM image of the Char-AP sample shows the surface morphology is smooth, no obvious micro-pores and micro-channels are observed on the char surface, and the most noticeable feature identified on the product char was the formation of particles over its surface (Fig. 12a). The size of the particles ranged from 50 to 500 nm in diameter from SEM image. The formation of particle structures suggests that the secondary pyrolysis reactions occur to form the carbon deposits during the VP process. SEM results for chars obtained under vacuum pyrolysis are shown in Fig. 12b. SEM analysis indicated that the surface of the char is clean and obvious micropores and microchannels are formed after pyrolysis under vacuum at 800 °C. The clean surface means no secondary pyrolysis reactions happen, which form carbon deposits on the char during AP process. The solid product of wood pins-fines gasified under CO_2 atmosphere (Fig. 12c) show its surface is etched by CO_2 at high temperature. Figure 12d shows the morphology of the AC obtained from AP char activated by CO_2 at 800 °C for 2 h. The image demonstrates micropores are formed after the activation. Figure 12e is the image of the AC from VP char activated by CO_2 at 800 °C for 2 h, it shows micropores and microchannels are formed and the surface of the AC is clean and neat. Figure 12f shows the image of the Char-VG-CO_2 process sample which is more porous than the chars or ACs from other processes, and confirms there are more micropores and microchannels observed on the char. The chars and AC samples from the wood dust were also examined using SEM, these samples from the wood dust exhibited similar morphologies to those from the wood pins-fines.

Wood-based biomass has been utilized as a sustainable precursor to produce activated carbons in the past decades, the reported data from the previous works are listed in Table 3 to compare with present results.

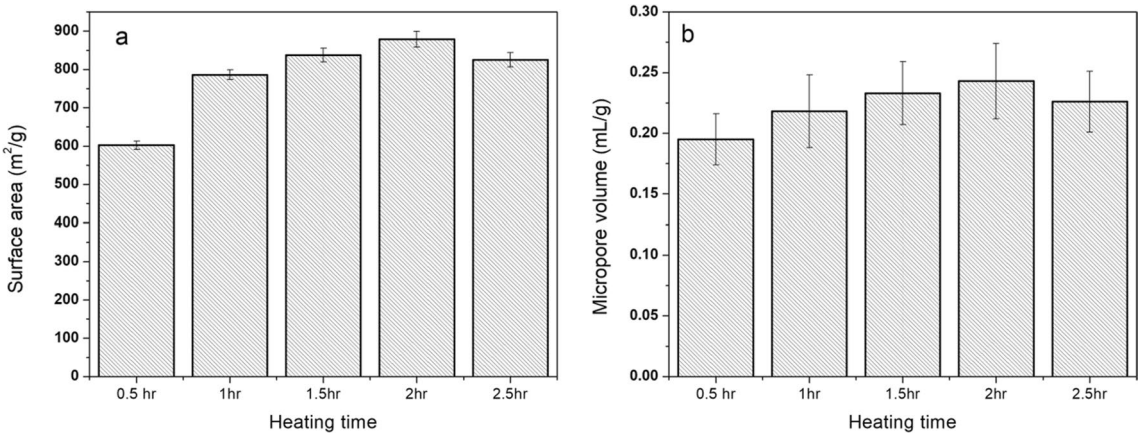

Fig. 11 Effect of heating time on surface area and micropore volume of char from vacuum CO_2 gasification of hardwood pins-fines at 800 °C (heating rate, 20 °C/min)

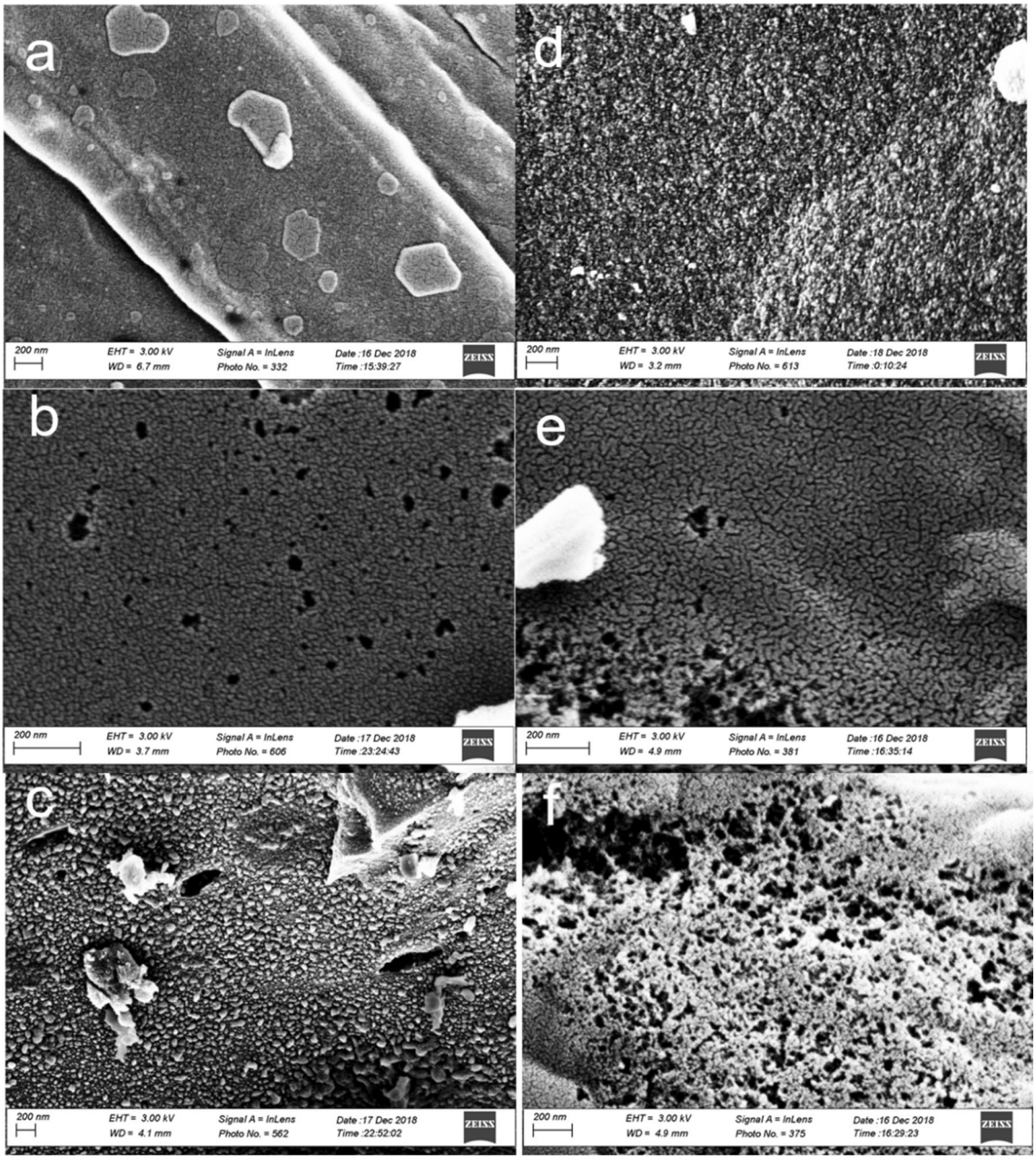

Fig. 12 Scanning electron micrographs of the chars and ACs from northern hardwood pins-fines prepared from different process at 800 °C for 2 h with heating rate of 20 °C/min: **a** Char-AP; **b** Char-VP; **c** Char-AG-CO_2; **d** AC-AP-CO_2; **e** AC-VP-CO_2; and **f** Char-VG-CO_2

4 Conclusions

Experimental studies on the preparation and characterization of chars and ACs from wood waste under vacuum pyrolysis and subsequent physical activation have been carried out. It is found that wood waste is a prospective starting material for the preparation of effective adsorbents. Effects of different pyrolysis/gasification processes on the chars and activated carbons have been investigated. The experimental results showed that the activated carbon pyrolyzed/gasified under vacuum while concurrently feeding in CO_2 at a temperature of 800 °C, a hold time of 2 h, and a heating rate of 20 °C/min resulted in the highest BET surface area and micropore volume of 878 m^2/g and 0.247 cm^3/g, respectively. Generally, increasing vacuum pyrolysis/gasification temperature reduces the yields of both chars and activated carbons. Too fast a heating rate will result in intense primary and secondary reactions and more carbon deposition in the pores of the char, consequently, promoting the formation of closed pores and hence a lower pore surface area. Too

Table 3 Carbonization and activation condition for different wood-based biomass to produce activated carbons

Raw material	Carbonization condition (°C/h)	Activation condition (°C/h)	BET surface area (m^2/g)	Total pore volume (cm^3/g)	Reference
Northern hardwood pins-fines	–	400–900 °C/1 h, vacuum, CO_2	78–855	0.197–0.243	Current work
Northern hardwood dust	–	400–900 °C/1 h, vacuum, CO_2	153–905	0.215–0.249	Current work
Pine sawdust	–	800 °C/2 h, CO_2	140–352	0.097–0.154	[59]
Pinewood	550 °C/4 h	900 °C/0.5–4 h, steam	426–902	0.321–0.749	[60]
Oak wood waste	450 °C	700 °C/1 h and 800 °C/2 h, CO_2	642–985	0.4113–0.6403	[61]
Mahogany sawdust	500 °C/1 h	800 °C/1 h, steam	516.3	–	[62]
Fir wood	450 °C/1.5 h	900 °C/7 h, steam	1009–1096	0.70–0.94	[63]
Wattle wood	400 °C/1 h	800 °C/5 h, CO_2	430–1030	0.21–0.56	[64]

long a vacuum pyrolysis/gasification heating time will also decrease the specific surface area of the activated carbon due to enlarging and collapsing pores.

Acknowledgements This work was supported by the USDA Forest Service through Grant Nos. 19-JV-11111124-053 and 19-JV-11111124-063. The authors would like to acknowledge Domtar Corp., North Carolina for providing wood pins-fines and wood dust samples for this study. Neil Gribbins and Timothy Ketelboeter at USDA Forest Products Laboratory provided editorial assistance.

References

1. Saleem J, Shahid U, Hijab M et al (2019) Production and applications of activated carbons as adsorbents from olive stones. Biomass Conv Bioref 9:775–802
2. Peng G, Gramm F, Ludwiga C, Vogel F (2015) Effect of carbon surface functional groups on the synthesis of Ru/C catalysts for supercritical water gasification. Catal Sci Technol 5:3658–3666
3. Bagheri S, Julkapli NM (2016) Effect of hybridization on the value-added activated carbon materials. Int J Ind Chem 7:249–264
4. Adegoke KA, Bello OS (2015) Dye sequestration using agricultural wastes as adsorbents. Water Resour Indus 12:8–24
5. Menendez-Diaz JA, Martin-Gullon I (2006) Types of carbon adsorbents and their production. In: Bandosz TJ (ed) Activated carbon surfaces in environmental remediation. Academic Press, New York, pp 1–47
6. Schlesinger WH, Bernhardt ES (2013) Chapter 5 the biosphere: the carbon cycle of terrestrial ecosystems. Biogeochemistry: an analysis of global change, 3rd edn. Academic Press, Boston, pp 135–171
7. Jahanban-Esfahlan A, Ostadrahimi A, Tabibiazar M, Amarowicz R (2019) A comparative review on the extraction, antioxidant content and antioxidant potential of different parts of walnut (*Juglans regia* L.) fruit and tree. Molecules 24:2133
8. Field CB, Behrenfeld MJ, Randerson JT, Falkowski P (1998) Primary production of the biosphere: integrating terrestrial and oceanic components. Science 281:237–240
9. Amirza MAR, Adib MMR, Hamdan R (2017) Preface. MATEC Web Conf 103:1–12
10. Agblevor FA, Besler S (1996) Inorganic compounds in biomass feedstocks. 1 Effect on the quality of fast pyrolysis oils. Energy Fuels 10:293–298
11. Dias JM, Alvim-Ferraz MC, Almeida MF, Rivera-Utrilla J, Sanchez-Polo M (2007) Waste materials for activated carbon preparation and its use in aqueous-phase treatment: a review. J Environ Manag 85:833–846
12. Falk B (1997) Opportunities for the woodwaste resource. For Prod J 47:17–22
13. Prairie Village KS (1998) Characterization of building-related construction and demolition debris in the United States. The U.S. Environmental Protection Agency Municipal and Industrial Solid Waste Division Office of Solid Waste, Prairie Village, Kansas, 1998.
14. Nelson L, Park S, Hubbe MA (2018) Thermal depolymerization of biomass with emphasis on gasifier design and best method for catalytic hot gas conditioning. BioRes 13:4630–4727
15. Hanks L (1977) Predicted cubic-foot yields of lumber, sawdust, and sawmill residue from the sawtimber portions of hardwood trees. Research Paper NE-380. USDA Forest Service, Northeastern Experiment Station, Upper Darby, Pennsylvania.
16. Ince PJ, McKeever DB (1995) Recovery of paper and wood for recycling: actual and potential. General Technical Report FPL-GTR88. USDA Forest Service, Forest Products Laboratory, Madison, p 13
17. Grigoriou AH (2003) Waste paper–wood composites bonded with isocyanate. Wood Sci Technol 37:79–90
18. Xiu S, Shahbazi A (2012) Bio-oil production and upgrading research: a review. Renew Sustain Energy Rev 16:4406–4414
19. Hata T, Vystavel T, Bronsveld P, De Hosson J, Kikuchi H, Nishimiya K, Imamura Y (2004) Catalytic carbonization of wood charcoal: graphite or diamond? Carbon 42:961–964
20. Yan Q, Li J, Zhang X, Zhang J, Cai Z (2019) Mass production of graphene materials from solid carbon sources using a molecular cracking and welding method. J Mater Chem A 7:13978–13985
21. Rosales-Calderon O, Arantes V (2019) A review on commercial-scale high-value products that can be produced alongside cellulosic ethanol. Biotechnol Biofuels 12:240
22. Shi K, Yan J, Menéndez JA, Luo X, Yang G, Chen Y, Lester E, Wu T (2020) Production of H2-rich syngas from lignocellulosic biomass using microwave-assisted pyrolysis coupled with activated carbon enabled reforming. Front Chem 8:3
23. Dąbrowski A, Podkościelny P, Hubicki Z, Barczak M (2005) Adsorption of phenolic compounds by activated carbon. A critical review. Chemosphere 58:1049–1070
24. Hayashi JI, Horikawa T, Takeda I, Muroyama K, Ani F (2002) Preparing activated carbon from various nutshells by chemical activation with K2CO3. Carbon 40:2381–2386
25. Machrouhi A et al (2019) Statistical optimization of activated carbon from Thapsia transtagana stems and dyes removal efficiency using central composite design. J Sci Adv Mater Devices 4:544–553

26. Şahin Ö, Saka C (2013) Preparation and characterization of activated carbon from acorn shell by physical activation with H_2O–CO_2 in two-step pretreatment. Bioresour Technol 136:163–168
27. Bae W, Kim J, Chung J (2014) Production of granular activated carbon from food-processing wastes (walnut shells and jujube seeds) and its adsorptive properties. J Air Waste Manag Assoc 64:879–886
28. Kawamoto H (2017) Lignin pyrolysis reactions. J Wood Sci 63:117–132
29. Libbrecht W, Vandaele K, De Buysser K, Verberckmoes A, Thybaut J, Poelman H, De Clercq J, Van Der Voort P (2015) Tuning the pore geometry ofordered mesoporous carbons for enhanced adsorption of bisphenol-a. Materials 8:1652–1665
30. Dufour A, Celzard A, Fierro V, Martin E, Broust F, Zoulalian A (2008) Catalytic decomposition of methane over a wood char concurrently activated by a pyrolysis gas. Appl Catal A Gen 346:164–173
31. Carrier M, Hardie AG, Uras U, Gorgens J, Knoetze JH (2012) Production of char from vacuum pyrolysis of South-African sugar cane bagasse and its characterization as activated carbon and biochar. J Anal Appl Pyrolysis 96:24–32
32. Plante P, Roy C, Chornet E (1988) CO gasification of wood charcoals derived from vacuum and atmospheric pyrolysis. Can J Chem Eng 66:307–312
33. Ismadji S, Sudaryanto Y, Hartono SB, Setiawan LE, Ayucitra A (2005) Activated carbon from char obtained from vacuum pyrolysis of teak sawdust: pore structure development and characterization. Bioresour Technol 96:1364–1369
34. Cao N, Darmstadt H, Roy C (2001) Activated carbon produced from charcoal obtained by vacuum pyrolysis of softwood bark residues. Energy Fuels 15:1263–1269
35. Cao NZ, Darmstadt H, Soutric F, Roy C (2002) Thermogravimetric study on the steam activation of charcoal obtained by pyrolysis of bark residue. Carbon 40:471–479
36. ASTM D4442-07 (2007) Standard test methods for direct moisture content measurement of wood and wood-based materials. ASTM Int., West Conshohocken
37. ASTM D1102-84 (2007) Standard test method for ash in wood. ASTM Int., West Conshohocken
38. Yan Q, Boardman CR, Cai Z (2020) Thermal stability of metal-lignin composites prepared by coprecipitation method. Thermochim Acta 690:178659
39. Leal GF, Ramos LA, Barrett DH, Curvelo AAS, Rodella CB (2015) A thermogravimetric analysis (TGA) method to determine the catalytic conversion of cellulose from carbon-supported hydrogenolysis process. Thermochim Acta 616:9–13
40. Yan Q, Li J, Zhang J, Cai Z (2018) Thermal decomposition of kraft lignin under gas atmospheres of argon, hydrogen, and carbon dioxide. Polymers 10:729
41. González-Díaz E, Alonso-López JM (2017) Characterization by thermogravimetric analysis of the wood used in Canary architectural heritage. J Cult Herit 23:111–118
42. Gašparovič L, Koreňová Z, Jelemenský L (2010) Kinetic study of wood chips decomposition by TGA. Chem Pap 64:174–181
43. Poletto M, Dettenborn J, Pistor V, Zeni M, Zattera AJ (2010) Materials produced from plant biomass. Part I: evaluation of thermal stability and pyrolysis of wood. Mater Res 13:375–379
44. Zghari B, Doumenq P, Romane A, Boukir A (2017) GC-MS, FTIR and 1H, 13C NMR structural analysis and identification of phenolic compounds in olive mill wastewater extracted from oued Oussefrou effluent (Beni Mellal-Morocco). J Mater Environ Sci 8:4496–4509
45. Awal A, Sain M (2011) Spectroscopic studies and evaluation of thermorheological properties of softwood and hardwood lignin. J Appl Polym Sci 122:956–963
46. Guo Y, Bustin RM (1998) FTIR spectroscopy and reflectance of modern charcoals and fungal decayed woods: implications for studies of inertinite in coals. Int J Coal Geol 37:29–53
47. Hajji L, Boukir A, Assouik J, Pessanha S, Figueirinhas JL, De Carvalho ML (2016) Artificial ageing paper to assess long term effects of conservative treatment. Monitoring by infrared spectroscopy (ATR-FTIR), X-ray diffraction (XRD) and Energy dispersive X-ray fluorescence (EDXRF). Microchem J 124:646–656
48. Emmanuel V, Odile B, Céline R (2015) FTIR spectroscopy of woods: a new approach to study the weathering of the carving face of a sculpture. Spectrochim Acta A Mol Biomol Spectrosc 136:1255–1259
49. Oh SY, Yoo DI, Shin Y, Seo G (2005) FTIR analysis of cellulose treated with sodium hydroxide and carbon dioxide. Carbohydr Res 340:417–428
50. Gronert S (2006) Evidence that alkyl substitution provides little stabilization to radicals: the C−C bond test and the nonbonded interaction contradiction. J Org Chem 71:7045–7048
51. Liu Q, Wang S, Zheng Y, Luo Z, Cen K (2008) Mechanism study of wood lignin pyrolysis by using TG–FTIR analysis. J Anal Appl Pyrolysis 82:170–177
52. Wang S, Wang K, Liu Q, Gu Y, Luo Z, Cen K, Fransson T (2009) Comparison of the pyrolysis behavior of lignins from different tree species. Biotechnol Adv 27:562–567
53. Kishimoto T, Uraki Y, Ubukata M (2006) Chemical synthesis of β-O-4 type artificial lignin. Org Biomol Chem 4:1343–1347
54. Zhao J, Wang X, Hu J, Liu Q, Shen D, Xiao R (2014) Thermal degradation of softwood lignin and hardwood lignin by TG-FTIR and Py-GC/MS. Polym Degrad Stab 108:133–138
55. Safdari MS, Rahmati M, Amini E, Howarth JE, Berryhill JP, Dietenberger M, Weise DR, Fletcher TH (2018) Characterization of pyrolysis products from fast pyrolysis of live and dead vegetation native to the Southern United States. Fuel 229:151–166
56. Zaman CZ, Pal K, Yehye WA, Sagadevan S, Shah ST, Adebisi GA, Marliana E, Rafique RF, Johan RB (2017) Pyrolysis: a sustainable way to generate energy from waste. Book: pyrolysis. InTech, London, pp 3–34. https://doi.org/10.5772/intechopen.69036
57. Yan Q, Toghiani H, Yu F, Cai Z, Zhang J (2011) Effects of pyrolysis conditions on yield of bio-chars from pine chips. For Prod J 61:367–371
58. Lua AC, Yang T (2004) Effects of vacuum pyrolysis conditions on the characteristics of activated carbons derived from pistachio-nut shells. J Colloid Interface Sci 276:364–372
59. Nowicki P, Pietrzak R (2010) Carbonaceous adsorbents prepared by physical activation of pine sawdust and their application for removal of NO_2 in dry and wet conditions. Bioresour Technol 101:5802–5807
60. Tseng RL, Wu FC, Juang RS (2003) Liquid-phase adsorption of dyes and phenols using pinewood-based activated carbons. Carbon 41:487–495
61. Zhang T, Walawender WP, Fan LT, Fan M, Daugaard D, Brown RC (2004) Preparation of activated carbon from forest and agricultural residues through CO_2 activation. Chem Eng J 105:53–59
62. Malik PK (2004) Dye removal from wastewater using activated carbon developed from sawdust: adsorption equilibrium and kinetics. J Hazard Mater 113:81–88
63. Wu FC, Tseng RL, Juang RS (2005) Preparation of highly microporous carbons from fir wood by KOH activation for adsorption of dyes and phenols from water. Sep Purif Technol 47:10–19
64. Ngernyen Y, Tangsathitkulchai C, Tangsathitkulchai M (2006) Porous properties of activated carbon produced from Eucalyptus and Wattle wood by carbon dioxide activation. Korean J Chem Eng 23:1046–1054